Synthesis of phosphonated comb-like copolymers and evaluation of their dispersion efficiency on CaCO 3 suspensions. Part I: Effect of an increasing phosphonic acid content

A. Tramaux, Nathalie Azema, Ghislain David, C. Negrell, A. Poulesquen, J. Haas, S. Remond

Synthesis of phosphonated comb-like copolymers and evaluation of their dispersion efficiency on $CaCO_3$ suspensions. Part I: Effect of an increasing phosphonic acid content

A. Tramaux [a], N. Azéma [a,*], G. David [b], C. Negrell [b], A. Poulesquen [c], J. Haas [c], S. Remond [d]

[a] C2MA, IMT Mines Ales, Univ Montpellier, 6 avenue de Clavières 30319 Ales, CEDEX, France
[b] Laboratoire Ingénierie et Architecture Macromoléculaire (IAM), Institut Charles Gerhardt de Montpellier, France
[c] Laboratoire de Physicochimie des Matériaux Cimentaires, Commissariat à l'Energie Atomique de Marcoule, Bagnols-sur-Cèze, France
[d] IMT Lille Douai, Univ. Lille, EA 4515 – LGCgE, F-59000 Lille, France

A B S T R A C T

Superplasticizers are admixtures widely used in the building industry for reducing the water content of concrete with a high fluidity and workability at short term, and for increasing concrete mechanical properties at long term. Polycarboxylates, which are synthetic comb-like copolymers, are the most used superplasticizer admixtures. In order to improve polycarboxylate efficiency and compatibility with use of mineral additives, high-sulfate concretes etc., various authors tried to change macromolecular architectures, including nature of anionic function. This paper is the first part of a study which presents synthesis of several macromolecular architectures of comb-like copolymers with phosphonic acid functions instead of classical carboxylic acid. Adsorption, dispersion and fluidification efficiency of these admixtures are evaluated on calcite suspensions in order to simulate early-age cement behavior. Moreover, settling behaviors are studied in order to characterize dispersion ability of synthetized polymers.

Keywords:
Superplasticizers
Calcite
Suspensions
Adsorption
Dispersion
Macromolecular structures

1. Introduction

Admixtures for cement based materials are commonly chemical used to modify or obtain certain properties [1,2]. Water reducers or plasticizers are among these admixtures and allow improving the workability of fresh concrete without increasing the water content, or decreasing the water content without changing workability. This control of fresh behavior improves the durability and mechanical properties of the hardened concrete [3] and allows specific concretes to be formulated, such as self-compacting concrete (SCC) [4].

Lignosulfonate were the first plasticizers used in concrete, and are derived from lignins in pulping industry. Then, polymelamine sulfonates (PMS) and polynaphtalene sulfonates (PNS) were developed [5]. However, these plasticizers are known to have a limited effectiveness and can potentially lead to retardation of the setting of cement paste [6]. The new generation is Polycarboxylates (PCE) referred to as High Range Water Reducers (HRWR) or superplasticizers. These superplasticizers are the most used in concrete industry and also the most studied in academic field [3,7–11]. In fact, the structure diversity of polycarboxylates allows various combinations of macromolecular parameters, which involves important modifications of their efficiency.

Polycarboxylates are comb-like copolymers with a succession of methacrylic acid units in the main chain, and a substitution of part of these methacrylic acid units by poly(ethylene glycol) methyl ether methacrylate, forming side chains from the main chain. The mode of action of superplasticizer consists of the so called "electro-steric" effect. This effect is the combination of electrostatic and steric repulsions, but many studies assume that steric repulsion dominates in the case of PCE [12]. The repulsion action of superplasticizers improves the dispersion of cement particles and avoids their agglomeration. Water trapped in agglomerates is released and can also contribute to increase the fluidity of cement paste.

One of the most interesting aspects of polycarboxylate is their structure diversity [13]. Many studies tried to synthetize copolymers with various molecular mass, side chain length, distance between two poly (ethylene glycol) arms (PEG) on the main chain, and even chemical nature of anchor function. It has been found that copolymers with similar side chain/main chain ratio have similar properties [14]. Increasing side chain length generally leads to higher dispersion capacities [15], but can also reduce adsorption efficiency when they are too long [16]. The more the main chain contains anionic functions, the higher its negative charge density; this often improves adsorption efficiency of macromolecules onto mineral surfaces [17]. Such investigations are needed to improve polycarboxylates efficiency, and their compatibility with cement based materials [5,11,18]. One of the most important parameter is the sulfate

* Corresponding author.
E-mail address: nathalie.azema@mines-ales.fr. (N. Azéma).

content of cement [2] which can lead to the consumption of the polymer to form organo-mineral phases [19], and/or to the decrease of the polymer adsorption by ionic competition phenomenon.

Fan et al. [20] added trialkoxysilanes functional groups in a polycarboxylate main chain, resulting in an improvement of compatibility with high sulfates-content mortars. Pourchet et al. [21] studied how repartition of monomers on backbone of the macromolecule influences dispersion behavior. These authors found that a gradient copolymer seems to be much more resistant to sulfate ions competition, compared to the random one. Various works were conducted in order to replace carboxylic acid function by another anionic function, for example a dicarboxylic or phosphonic acids [22,23]. These new macromolecular structures reveal a good sulfate resistance.

The understanding of involved phenomena on cement remains difficult due to the complexity of cementitious materials. In fact, cement paste is a multiphase material subjected to the hydration reactions. Model materials are commonly used to simplify the studies and to avoid the reactivity of cement [24–26]. Mikanovic and Jolicoeur [27] found that calcite ($CaCO_3$) suspensions exhibit colloidal properties very similar to those of cement pastes at early-ages and can be a suitable model system to simulate the early-age behavior of cement.

The aim of this paper is to study the influence of macromolecular structure of synthesized comb-like copolymers on their adsorption and dispersion efficiencies. Phosphonic acid content and statistical or bloc structures are regarded and their impact on adsorption investigated by TOC measurements, on dispersion by rheology and settling measurements.

2. Materials and methods

2.1. Material

Calcite was provided by Omya Company, referred as “Calcite Omya BL”. Structure of this calcite was analyzed by XRD using diffractometer Bruker D8 advance and by energy dispersive X-ray microscopy using FEI QUANTA 200 FEG high resolution environmental SEM. Calcite characterization is given in Section 3.2.

2.2. Sample preparation

In a beaker with magnetic stirrer, aqueous solution of synthetized polymer is introduced, and the total amount of liquid is completed with limewater freshly prepared. The pH of the limewater (12.8) is close to that of interstitial solution of cement paste, and its ionic strength is about 66 mmol/L. Note that this model solution does not exactly mimic Ca^{2+} concentration of cement paste because there are no source to replenish calcium ions through dissolution from clinker phases. Calcite is finally added. Volume of polymer solution is calculated according to the dosage targeted, which is the mass of dry polymer over the mass of calcium carbonate in the suspension. For this initial suspension, total amount of liquid added is calculated in order to keep constant water to solid ratio (W/S = 0.5) which corresponds to solid mass and volume fractions (respectively 66.66 wt% and 43 vol%) commonly used in concrete industry. This suspension is kept under magnetic stirring for at least 10 min before being diluted according to analysis requirements.

2.3. Chemical synthesis

2.3.1. Chemicals

Poly(ethylene glycol) methyl ether methacrylate of 950 g/mol ($MAPEG_{950}$), cyanoisopropyl dithiobenzoate (CIDB), 4,4′-Azobis (4-cyanovaleric acid) (ACVA), methacrylic acid (MAA) and methanol (MeOH) were purchased from Sigma-Aldrich. Dimethoxyphosphorylmethyl methacrylate (MAPC1) was purchased from Specific Polymers. Thioglycolic acid (TA) was purchased from Acros. Trimethylsilyl bromide (TMSBr) was purchased from Fluka Analytical and 2,2-Azobisisobutyronitrile (AIBN) was purchased from Fluka Chemika. Reagents were used as received, without any further purification.

2.3.2. Chemical characterization

^1H and ^{31}P NMR spectra were recorded in deuterated chloroform with a 400 MHz NMR spectrometer from Bruker Company. Steric exclusion chromatography analyses were carried out with a triple-detection GPC from Agilent Technologies equipped with a detector suite composed of a PL0390-0605390 LC light scattering detector with two diffusion angles (15° and 90°), a PL0390-06034 capillary viscometer, and a 390-LC PL0390-0601 refractive index detector. Two PL1113-6300 ResiPore 300 × 7.5 mm columns thermostated at 35 °C were used with an eluent flow of 0.8 mL/min. Columns were calibrated with polymethylmethacrylate (PMMA) standards. Steric exclusion chromatography (SEC) analyses were performed for the block copolymer in dimethylformamide (+0.1% of LiBr) with a small amount of toluene as flow rate marker.

2.3.3. Synthesis procedures

Copolymers were obtained by two synthesis routes: three statistical copolymers were prepared by conventional radical copolymerization, using ACVA as water-soluble initiator and thioglycolic acid as chain transfer agent. These copolymers differ by their anionic moieties: statistical PCE has 100% of carboxylic acids, statistical PCE-15P has half of carboxylic and half of phosphonic acids, and statistical PCE-30P has only phosphonic acid units. The block copolymer, named block PCE-30P, was prepared by Reversible Addition Fragmentation Transfer (RAFT) copolymerization, using AIBN as initiator and cyanoisopropyl dithiobenzoate (CIDB) as RAFT agent. Copolymers were first synthesized, dried, and then solubilized in distilled water in order to reach a 100 g/L concentration. Finally, accurate mass concentrations of these aqueous solutions were determined with thermobalance analysis.

2.3.4. Monomer preparation (MAPC1(OMe) hydrolysis)

Procedure for a typical hydrolysis: in a 250 mL three-neck round bottom flask, 3 g of MAPC1(OMe) (14.42 mmol) and 100 mL of anhydrous dichloromethane are introduced. The mixture is kept under nitrogen flux, in order to be in dry conditions. 5.7 mL of TMSBr (43.27 mmol, 3 eq.) are added dropwise with a dropping funnel. After 24 h of reaction, dichloromethane is eliminated and 100 mL of methanol are added for 3 h. Methanol is then eliminated, and the product is dried under vacuum (viscous orange oil). Total conversion is checked with ^{31}P NMR, whose signal is shifted from 24.5 ppm for MAPC1(OMe) to 19.4 ppm for MAPC1(OH).

2.3.5. Copolymers synthesis

2.3.5.1. Statistical copolymers synthesis. The statistical copolymer synthesis is similar to that described by Chougrani et al. [28] concerning the synthesis of statistical copolymers from MMA and MAPC1. Authors evidenced the statistical structure by calculating the reactivity ratios of both monomers.

X moles of methacrylic acid, Y moles of MAPC1(OH), Z moles of $MAPEG_{950}$, thioglycolic acid and distilled water are introduced in a 250 mL three-neck round bottom flask and kept under nitrogen flux (see Table 1). The mixture is heated at 70 °C and 1% of ACVA (according to moles of monomers) is added to the solution. After 24 h of reaction, solution is cooled and complete conversion is checked with ^1H NMR analysis. Water is then eliminated by lyophilization. Copolymers are collected as white powder and finally dried under vacuum until constant mass.

2.3.5.2. Block copolymer synthesis. The synthesis of block copolymer was obtained by RAFT, according to the procedure already described by

Table 1
Amount of reactants used for random copolymers synthesis.

Statistical copolymers						
Reference	Methacrylic acid mmol	MAPC1 (OH) mmol	$MAPEG_{950}$ mmol	Thioglycolic acid mmol	ACVA mmol	Water mL
PCE	12.99	–	30.33	0.76	1	60
PCE-15P	6.38	6.38	29.79	0.85	0.4	40
PCE-30P	–	17.94	42.18	1.11	0.8	140

Cannicionni et al. [29] concerning the RAFT polymerization of MAPC (OMe).

Block PCE-30P was obtained by RAFT copolymerization using CIDB as RAFT agent. The first step is the MAPC1(OMe) macroinitiator synthesis. The second is the addition of $MAPEG_{950}$ leading to MAPC1(OMe)-block-$MAPEG_{950}$ copolymer. The final step is the hydrolysis of MAPC1 (OMe) moieties on the macromolecule.

The first step corresponds to MAPC1(OMe) macroinitiator synthesis. MAPC1(OMe) (10.21 g, 49.09 mmol), CIDB (0.563 g, 2.54 mmol), AIBN (0.134 g, 0.816 mmol) and DMF (35 mL) are introduced in a round bottom flask. The mixture is kept under argon flux and heated at 70 °C. After precisely 6 h, reaction is stopped by immersing the flask in liquid nitrogen. ^{1}H NMR confirmed 80% monomer conversion, which enabled avoiding termination reactions. In order to remove remaining monomer, solution is poured in a large volume of cooled diethyl ether. The red precipitate is filtered, then washed with diethyl ether, before being dried under vacuum until constant mass.

The second step corresponds to MAPC1(OMe)-block-$MAPEG_{950}$ synthesis. MAPC1(OMe) macroinitiator (1.7 g, 0.532 mmol, Mn = 3200 g/mol), $MAPEG_{950}$ (18.2 g, 19.16 mmol), AIBN (23 mg, 0.14 mmol) and DMF (50 mL) are introduced in a round bottom flask. The mixture is kept under argon flux and heated at 70 °C. After precisely 6.25 h, reaction is stopped by immersing the flask in liquid nitrogen. ^{1}H NMR confirmed 80% monomer conversion. In order to remove remaining monomer, solution is poured in a large volume of cooled diethyl ether. The pink precipitate is filtered, and then washed with diethyl ether, before being dried under vacuum until constant mass.

The final step corresponds to hydrolysis of $P(OMe)_2$ moieties of MAPC1(OMe)-block-$MAPEG_{950}$. MAPC1(OMe)-block-$MAPEG_{950}$ (14.4 g, 0.37 mmol, Mn = 45,000 g/mol) is dissolved in dry dichloromethane and kept under nitrogen flux. TMSBr (1.54 g, 10.08 mmol) is added dropwise with a dropping funnel. After 24 h of reaction, dichloromethane is eliminated and methanol (200 mL) is added for 3 h. Methanol is then eliminated, and the product is dried under vacuum until constant mass. Total conversion is checked with ^{31}P NMR, whose signal is shifted from 21 ppm to 17.7 ppm for MAPC1(OH) moieties.

NMR data (Fig. 1).

Statistical PCE: ^{1}H (NMR 400 MHz, δ): 4.1 [2H,H_d]; 3.6 [4H, H_f and 2H, H_e]; 3.45 [3H,H_g]; 2.1-1.6 [2H, $H_b + H_{b'}$]; 1.2-0.7 [3H, $H_a + H_{a'}$].

Statistical PCE-15P: ^{1}H (NMR 400 MHz, δ): 4.0 [2H,H_d and 2H,H_h]; 3.6 [4H, H_f and 2H, H_e]; 3.45 [3H,H_g]; 2.1-1.5 [2H, $H_b + H_{b'} + H_{b''}$]; 1.2-0.6 [3H, $H_a + H_{a'} + H_{a''}$]; ^{31}P NMR (161.6 MHz, δ) 16.8 [**P**(O)$(OH)_2$].

Statistical PCE-30P: ^{1}H (NMR 400 MHz, δ): 4.1 [2H,H_d and 2H,H_h]; 3.6 [4H, H_f and 2H, H_e]; 3.45 [3H,H_g]; 2.1-1.6 [2H, $H_b + H_{b'}$]; 1.1-0.6 [3H, $H_a + H_{a'}$]; ^{31}P NMR (161.6 MHz, δ) 17.1 [**P**(O)$(OH)_2$].

Block PCE-30P: ^{1}H (NMR 400 MHz, δ): 4.1 [2H,H_d and 2H,H_h]; 3.6 [4H,H_f and 2H,H_e]; 3.45 [3H,H_g]; 2.1-1.6 [2H, $H_b + H_{b'}$]; 1.1-0.7 [3H, $H_a + H_{a'}$]; ^{31}P NMR (161.6 MHz, δ) 17.7 [**P**(O)$(OH)_2$].

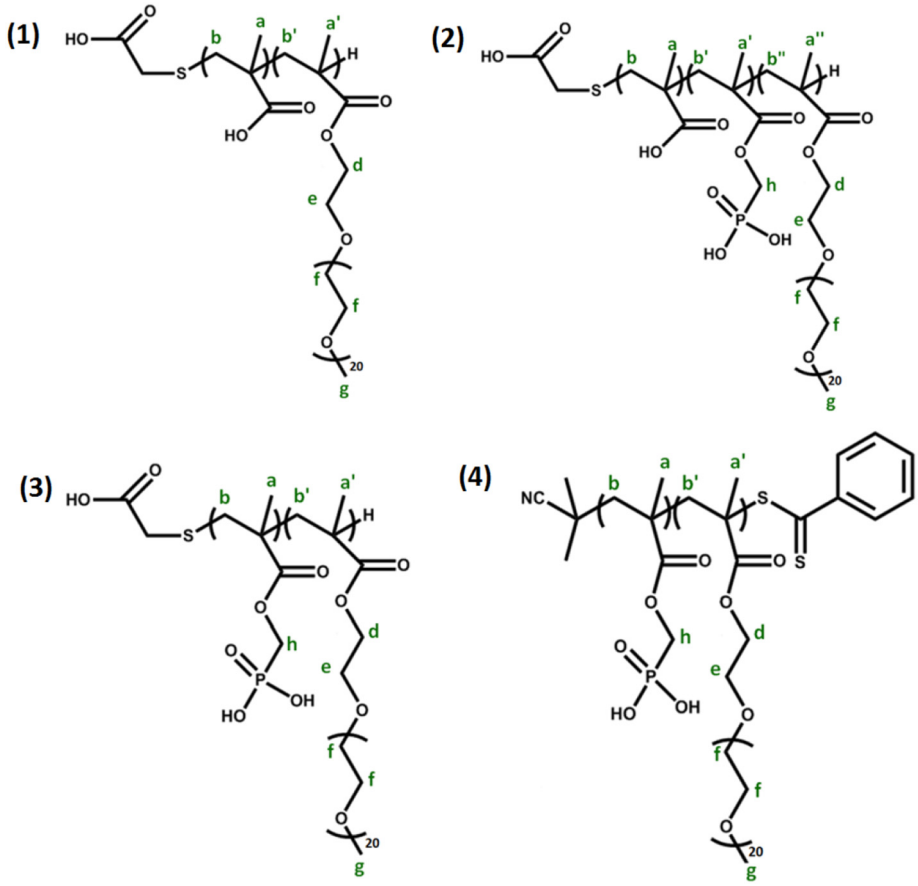

Fig. 1. Chemical formula of Statistical PCE (1), Statistical PCE-15P (2), Statistical PCE-30P (3) and Block PCE-30P (4).

2.4. Physico-chemical and granular characterizations

2.4.1. Adsorption of superplasticizers

Adsorption measurements were performed using Vario cube TOC (Total Organic Carbon) analyzer from Elementar. The aim of these measurements is to determine the adsorbed amount of copolymer. Concentration of superplasticizer in samples is determined after subtraction of the "blank" area value, and amount of copolymer adsorbed is calculated from difference between amount initially added in the sample and amount determined by TOC analysis. Note that when superplasticizer is added to limewater, no precipitate is observed (which might be cause by insoluble polymer-Ca^{2+} complex). Calcite is then added to a clear solution which leads to believe that a loss of polymer in interstitial solution comes from adsorption phenomenon.

Samples are prepared as follows: 50 g of initial suspension are prepared and stirred for at least 10 min. Suspensions are centrifuged and supernatants are filtered through a 0.45 μm PTFE filter. 4 mL of this solution are pipetted and completed to 20 mL with deionized water. A drop of sulfuric acid is added in TOC tube before analysis, in order to avoid the formation of small particles of $CaCO_3$ that systematically occurs in an alkali solution including Ca^{2+} ions in contact with CO_2 from air.

For every series of analysis, several standards (ethanol aqueous solutions of known concentration), one standard of the copolymer of interest (of accurate concentration, approximately 5 g/L) and a "blank" sample (initial suspension without any copolymer added) are prepared.

2.4.2. Dispersion and granular characterizations

2.4.2.1. Dispersion characterization. Dispersion state of suspension studied has been indirectly characterized by settling measurements with a Turbiscan MA 2000 analyzer from Formulaction Company. This device can detect light flux transmitted (T) and backscattered (BS) from a near IR source ($\lambda = 860$ nm) as a function of height of a cylindrical glass cell (15 mm diameter and 110 mm height) with a step of 40 μm. According to following relationships, light intensity measurements are linked to d, the mean diameter of particles and Φ the solid volume fraction of sample (%):

$$Tr = e^{\frac{-r_i}{\lambda^*}} \quad (1)$$

$$BS = \frac{1}{\sqrt{\lambda^*}} \quad (2)$$

With

$$\lambda = \lambda^*(1-g) \quad (3)$$

$$\lambda^* = \frac{2d}{3\Phi(1-g)Q_s} \quad (4)$$

Tr and BS are respectively the intensity of transmitted and backscattered light (%), r_i is the internal radius (μm) of the measurement cell, λ^* is the photon transport length (μm) [30]. Q_s and g are two parameters from the Lorentz-Mie theory, respectively the scattering efficiency factor and the asymmetry factor. Evolution of Tr and BS as a function of time give information about dispersion/agglomeration phenomena and migration of particles.

In order to observe sedimentation behaviors in a reasonable analysis time, a 3/10 dilution factor with limewater is performed before settling measurements (leading to 20 wt%, which correspond to $W/S = 4$). After at least 5 min of magnetic stirring, 7 mL of diluted suspension are pipetted into the Turbiscan cell. Turbiscan analyses last 30 min, with a scan every minute.

2.4.2.2. Scanning electron microscopy and particle size distribution. SEM observations have been realized with a Quanta FEG 200 device, from the FEI Company. Two kinds of preparations have been employed for calcite SEM observations: calcite powder deposed on an aluminum stub whose surface is covered with an adhesive conductive carbon tab, or observation of a drop of calcite suspension on a glass slide according to the method described in Autier et al. [31].

Particle size distributions were measured using a LS 13320 laser granulometer from Beckman Coulter Company. Optical model used is based on refractive index of calcite with a real part 1.65 and imaginary part of 0.01. The time of analysis was set at 90 s, and data are displayed as a volume percentage curve, normalized to 100%. Carrier liquid employed was limewater.

2.4.2.3. Specific surface area measurement. The specific surface area was determined from nitrogen adsorption measurement using the BET model with a Tristar II device from Micromeritics Company.

2.4.3. Calcite suspensions rheology

Rheological measurements were carried out using an experimental Couette rheometer AR2000 ex from TA instruments equipped with a four blades vane geometry. Calcite suspensions were prepared with water to solid (W/S) ratio of 0.36 and a superplasticizer dosage of 0.05%. The measurements consist of a pre-shear phase at 250 s^{-1} during 30 s followed by a resting time of 30 s. The viscosity is then measured at a constant shear rate. Then, acquisition consists in a constant shear at 100 s^{-1} during 10 min. η_{10} is the average viscosity from 10 min of analysis.

3. Results and discussion

3.1. Macromolecular synthesis and characterizations

According to procedures described in 2.3.3., four copolymers have been synthesized. General synthesis strategy of statistical and block copolymers are presented on Scheme 1.

In a previous work [32], it was shown that molecular mass, side chain length and monomer ratios are macromolecular parameters that may have an effect on both adsorption and dispersion efficiencies of superplasticizers. These authors show that 70% of poly(ethylene glycol) methyl ether methacrylate in the chain reveals better global efficiency with cement pastes. This structure was selected as reference for the present work. Its molecular mass was about 35,000 g/mol.

Table 2 presents structural parameters of the synthetized superplasticizers studied. All synthesized copolymers show almost same DPn and Mn. In each synthesis, commercial monomer MAPEG of 950 g/mol has been employed, warranting 20 units of PEG in each side chain. Statistical PCE has the same structure as a conventional polycarboxylate, it is a random copolymer with 30% of methacrylic acid and 70% of $MAPEG_{950}$ on carbon backbone. The second superplasticizer, statistical PCE-15P, is a terpolymer, whose structure is almost the same as statistical PCE with a substitution of half of methacrylic acid by MAPC1(OH) moieties. Statistical PCE-30P is the same as statistical PCE, with a total substitution of carboxylic acid moieties by MAPC1(OH). All these copolymers are random and the chain extremity is assumed to be derived from thioglycolic acid, chain transfer agent used for molar mass control. Block PCE-30P has exactly same structural parameters as statistical PCE-30P but it differs in the monomer repartition on the carbon backbone because it is a block copolymer. For this one, chain extremity is assumed to be derived from CIDB, the RAFT agent required for this diblock structure. To our knowledge, only one paper deals with the synthesis of block copolymers for superplasticizer study [33].

For the three random copolymers synthesis, a reaction time of 24 h has been employed in order to ensure total conversion. Opening of all monomers double bonds is systematically checked with ^1H NMR. For the block copolymer, conversion is stopped at 80% in order to avoid

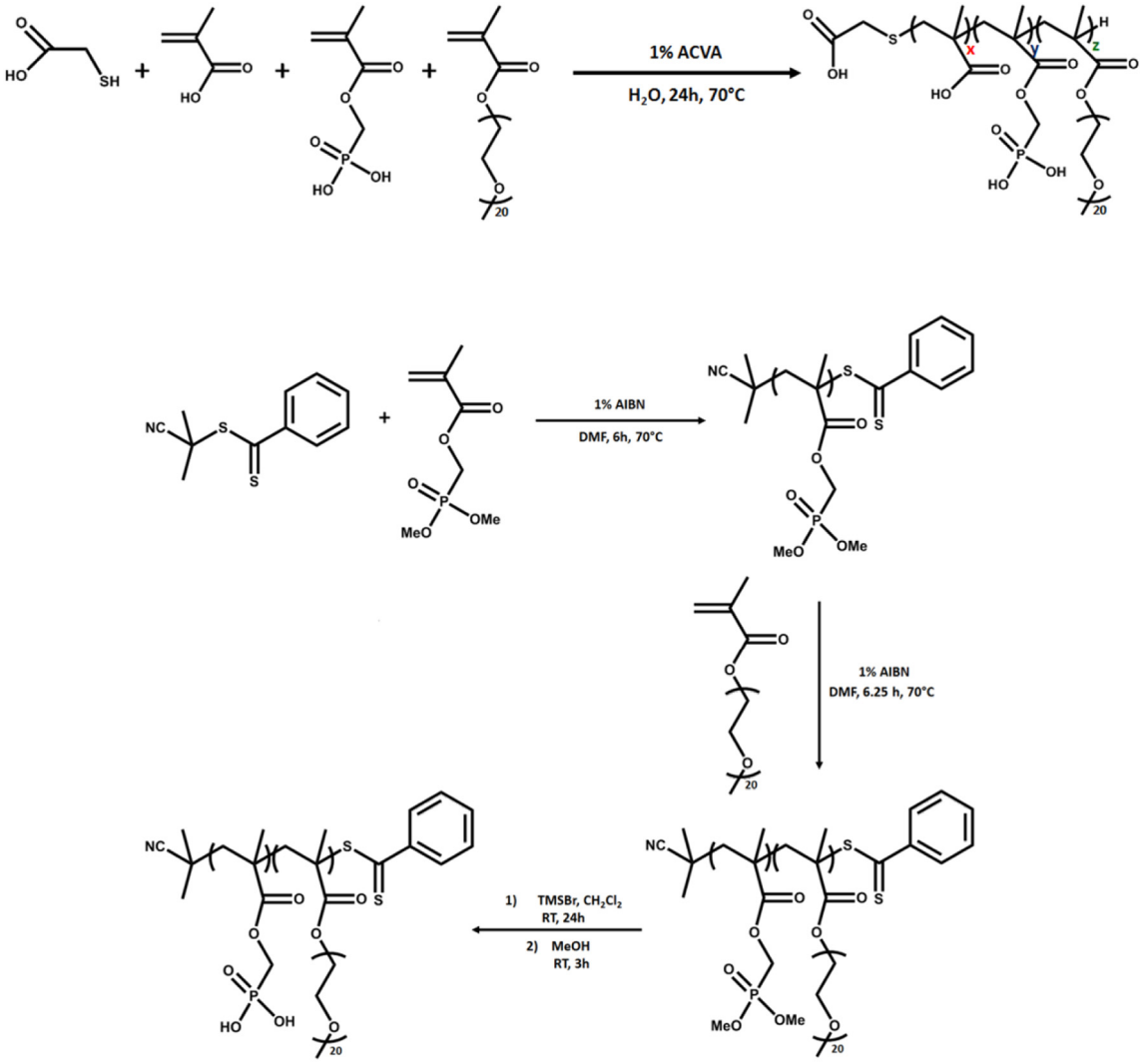

Scheme 1. General strategy for random and block copolymers synthesis.

termination reactions. Although calculation of Mn would be possible thanks to the integral of the signal of CH_2 in alpha position from sulfur atom in the thioglycolic acid moiety, this chemical shift is assumed to be 3.3–3.5 ppm. Because this spectral range displays NMR signals whose intensities are higher than this CH_2 of interest, molecular mass can't be calculated with NMR data.

3.2. Granular characterization of powder and suspension of calcite

BET specific surface area of calcite powder was measured at 1.25 m^2/g. Zeta potential of calcite particles has been determined by Pourchet et al. [34] at 20 mV in presence of 21 mmol/L of Ca^{2+} (same concentration as in limewater). It indicates weakly dispersed regime according to Riddick scale [35]. Moreover, surface characterizations were complemented with SEM observations and laser granulometry measurements. First, calcite powder and suspension have been observed with SEM, according to procedure described in 2.4.2. These results are presented in Fig. 2.

We can notice that all samples are polydispersed with a particle size range from 0.1 μm to 20–30 μm. Particles present a monomorphic angular shape, finest particles agglomerated onto larger particles are visible. No significant difference is observed between powder and suspension preparation. SEM observations are also confirmed by laser granulometry acquisitions revealing a main mode at 8 μm and a size spreading from 0.3 to 30–40 μm.

Table 2
Structural parameters of synthetized copolymers. *Calculated from reactants quantities employed. **For this diblock copolymer, the first block has 14 MAPC1(OH) units and the second block has 38 $MAPEG_{950}$ units. ***Calculated from GPC analysis of block copolymer before hydrolysis of $PO(OMe)_2$ moieties.

Reference	Monomer content in copolymers			DPn*	Mn* (g/mol)
	MAA	MAPC1(OH)	$MAPEG_{950}$		
Statistical PCE	30%	–	70%	57	38,500
Statistical PCE-15P	15%	15%	70%	50	35,000
Statistical PCE-30P	–	30%	70%	52	37,000
Block PCE-30P	–	30%	70%	52**	38500***

3.3. Adsorption of superplasticizers

TOC analyses allow determination of adsorbed copolymers amount, expressed as milligrams of adsorbed copolymers per grams of calcite. Direct correlation between quantity of adsorbed polymer and fluidification efficiency has been reported for similar macromolecular architectures [20,21]. The more the mass of admixture is adsorbed onto mineral surfaces, the more the macromolecules might participate to particle dispersion.

Adsorption ability of a superplasticizer depends on its macromolecular architecture, such as molecular mass or side chain length, but key parameters are both chemical nature [36] and distribution [20] of anionic functions, which directly influence the anchoring potential.

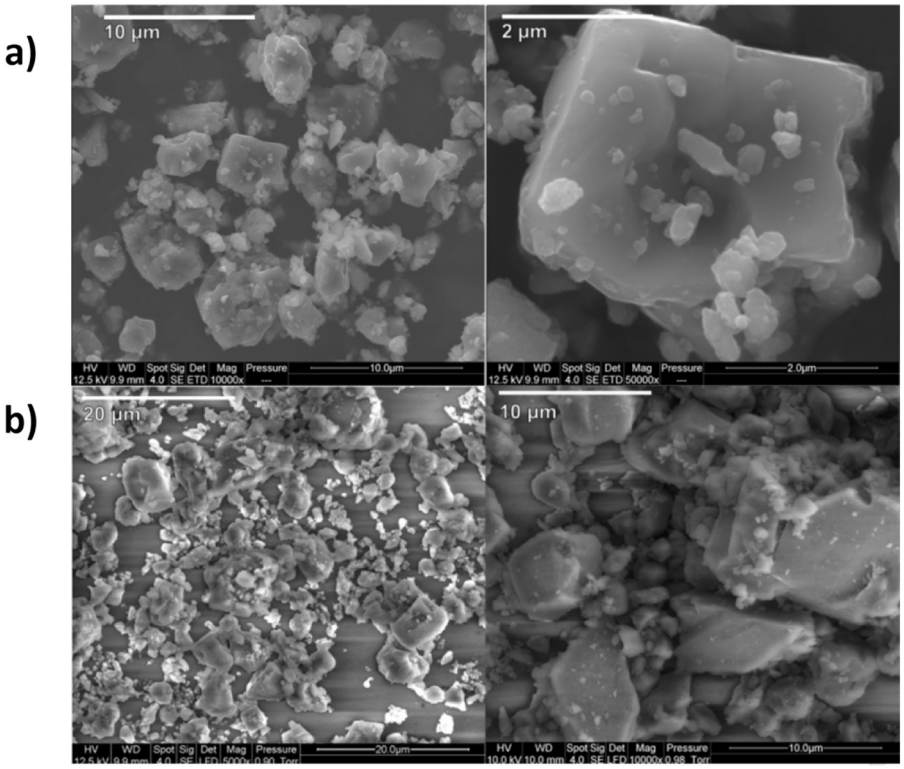

Fig. 2. SEM micrographs of dry calcite powder (a) and concentrated calcite suspension (b).

Fig. 3 presents the amount of adsorbed copolymer for superplasticizer dosage 0.01 to 1%, in limewater. Dosages >1% have not been possible due to the small quantities of synthetized polymers in regard to the large number of experiments realized in this work. In this context, saturated adsorption could not be reached. In this alkali solution (pH: 12.8), acid functions are assumed to be fully deprotonated, leading to better adsorption. As expected, superplasticizer adsorption increases with the dosage employed. We can notice that under dosage of 0.2%, polymer structure has a little influence on adsorption efficiency.

However, for dosages higher than 0.2%, an increase of phosphonic acid content leads to a decrease of quantity of polymer adsorbed (1.52 mg/g of calcite for statistical PCE-15P and only 1.14 mg/g of calcite for statistical PCE-30 - all measurements have been duplicated 3 times to obtain a reproductibility of ±0.007 mg/g of calcite). These results could be due to possible formation of water-soluble calcium complexes (phosphonates are excellent chelators for Ca^{2+}) which could affect adsorption behavior when phosphonic acid groups increase [37]. Note that the saturation plateau is also influenced by polymer structure and is reached respectively at 0.5%, 0.2% and not reached for statistical PCE-15P, statistical PCE-30P and statistical PCE. This plateau is usually obtained for conventional PCEs at approximately 0.5% for cement pastes but often absent for mineral suspensions [38].

On the other hand, block PCE-30P seems to adsorb in higher amount than all other copolymers; this result may be due to a very different macromolecular architecture. In fact, adsorbed copolymers are supposed to have a "blob" conformation, whose diameters are assumed to be close to the radius of gyration of macromolecules in solution [39]. This diameter depends on superplasticizer affinity for the liquid; in very good solvent conditions, copolymers should have an optimal radius of gyration. Maybe block PCE-30P has less affinity for limewater than other statistical copolymers, due to its diblock structure. This could possibly result in a more compact conformation, increasing its adsorption amount per grams of calcite particle. A similar observation has been found by Lemaître [40] for poly(acrylic acid) linear homopolymers.

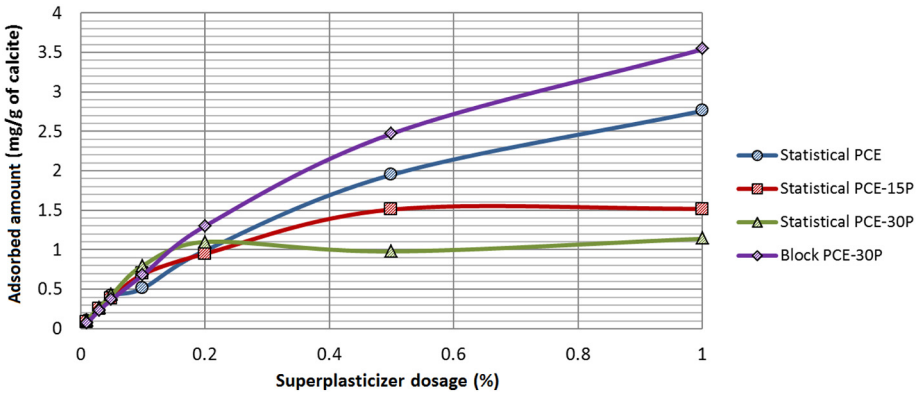

Fig. 3. Adsorbed amount onto calcite in limewater as a function of superplasticizer dosage.

3.4. Impact of superplasticizers macromolecular structures on dispersion state

Study of settling behaviors performed by Turbiscan MA 2000 allows us to qualify and quantify dispersion state of suspension.

Two zones in the sedimentation column can be studied: sediment in formation and supernatant (which can be clear, turbid or fully opaque). These two zones, according to their turbidity, can be studied either with transmission, or with backscattered profiles (Section 2.4.2).

Two kinds of general evolutions are observed: when calcite is not admixture, or at low superplasticizer dosage, a visible clarification of a turbid (but not opaque) supernatant is noticed on transmission profiles evolutions (indicated by red arrow on Fig. 4(a)), and a sediment front evolution can be clearly followed as a function of time on backscattered profiles (indicated by blue arrow on Fig. 4(b)).

But, when dosage is higher, particles settle more slowly due to a stabilization of the system. In this case, suspension column remains opaque all along its height (Fig. 4(c)). No sediment front evolution is observed, but just a clarification phenomenon of opaque supernatant formed can be observed on backscattered profiles (Fig. 4(b)).

3.4.1. Finest particles dispersion

In order to quantify dispersion efficiency of superplasticizer macromolecular structures and dosages, one can propose to measure the mean transmission percentage of supernatant after 30 min of settling. Used as a dispersion index, this parameter is named T_{30} and is related to the amount of finest particles dispersed and remaining in suspension at the top of sedimentation column, while the larger ones have settled down to the bottom (opaque supernatants can't be analyzed by this way). To define the term "finest particles", particle size distribution of supernatant has been measured by laser granulometry. Minimum and maximum diameters are respectively at 0.065 and 8 μm with two principal modes at 0.3 and 1.7 μm. Note that the d_{max} (8 μm) corresponds to the principal mode of the global particle size distribution of $CaCO_3$ (Section 3.2).

Fig. 5 shows values of T_{30} versus superplasticizers and their dosages. As a general trend, addition of superplasticizer with a dosage above 0.05%, leads to an opaque supernatant indicating a higher rate of finest particle dispersion. On Fig. 5 inlet, for lowest dosages and for all superplasticizers, better dispersion ability seems to be observed when phosphonic acid content increases. By contrast, block copolymer structure (block PCE-30P) has less dispersion efficiency potentially linked to adsorbed molecule conformation.

3.4.2. Impact of superplasticizers on rheological behavior

One of the most visible effects of adding superplasticizers in calcite suspensions is fluidification: the more the quantity of copolymer employed, the lower the viscosity. There is a common understanding that viscosity decreases when dispersion state is improved. At low dosage, a calcite suspension prepared with a W/S ratio of 0.36 can't flow under its own weight whereas at high copolymer dosage, the material reaches a viscosity almost as low as water and can be easily poured in a beaker, for instance. To quantify superplasticizers efficiency, rheological experiments were conducted at 0.05% dosage.

In order to compare similar values for each system, the sample average viscosity during all analysis time ($t = 600$ s) has been calculated in Fig. 6; in addition, a fluidification efficiency factor has been calculated from the ratio of the sample viscosity divided by unadmixtured suspension viscosity, named here "f". Fig. 6 shows that addition of superplasticizer results in an important decrease in viscosity, compared to unadmixtured calcite suspensions.

As a general trend, we can notice the more superplasticizer includes phosphonic acid, the lower is the viscosity. Among all copolymers, statistical PCE-30P shows the best efficiency, reducing the viscosity by a factor 12. Nevertheless, the block copolymer, despite its high adsorption efficiency, divides only by a factor 2 the viscosity. This may probably mean that the block copolymer due to its diblock structure, has less affinity for limewater and thus has a lower radius once adsorbed on particle surface. The weak steric hindrance of such compact conformation should result in a lower effect on dispersion state of particles (in accordance with previous results in 3.4.1.), leading to poor fluidification efficiency. Lemaître and Chen have also found that, in some conditions, an increased adsorption amount of PAA homopolymers results in a poor dispersion efficiency on $BaTiO_3$ particles, probably owing to a globular conformation of PAA at low pH [40].

Adsorption, finest particles dispersion and fluidification results can be correlated: block PCE-30P needs the highest dosage to disperse finest particles, and is also the least effective to fluidize suspensions. On the contrary, statistical PCE-30P requires the lowest dosage to disperse finest particles (get $T_{30} = 0$) and can fluidize efficiently calcite suspensions. Moreover, statistical PCE-30P and PCE-15P, which are the two copolymers leading to a better dispersion state, reached an adsorption saturation plateau at 0.5% dosage (see Fig. 3).

3.4.3. Stability index to quantify superplasticizer dispersion ability

When suspension is fully opaque, dispersion can't be characterized by transmission profiles (T_{30} index) but only by backscattered profiles

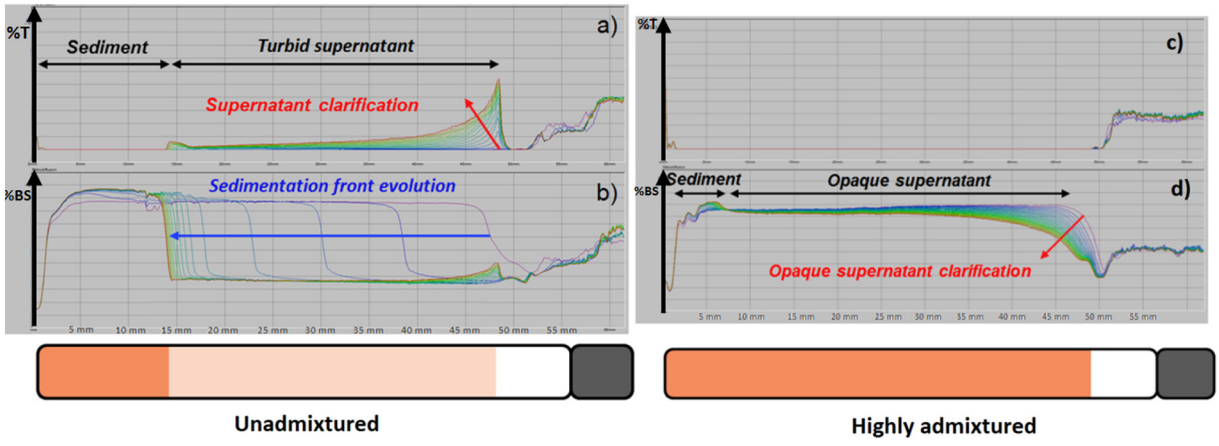

Fig. 4. Examples of Turbiscan profiles evolution as a function of column height (mm) for turbid (a) and opaque (c) supernatant on transmitted light intensity (T) and for instable (b) and more stable (d) sedimentation column on backscattered light intensity (BS).

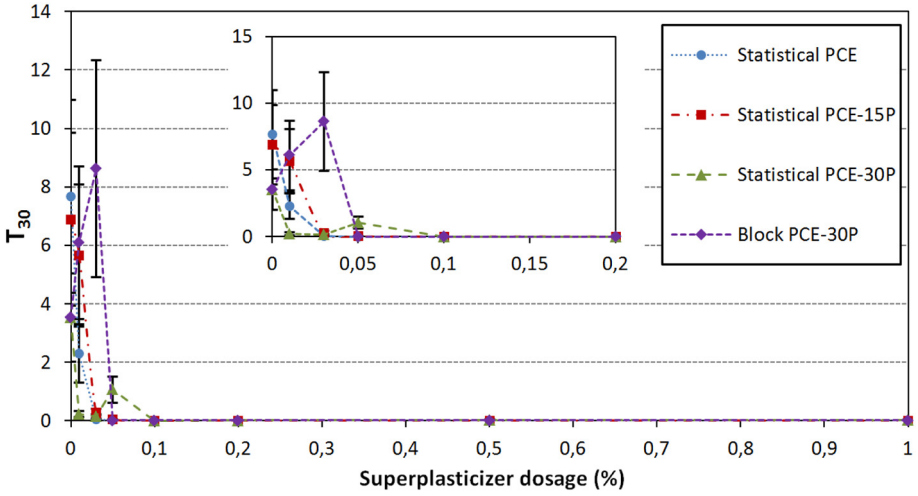

Fig. 5. Mean transmission percentage in supernatant (T_{30}) as a function of superplasticizer dosage in limewater.

evolution. By this way, dispersion of all particles is taken into account not only the finest ones suspended in supernatant. Hence another parameter has been defined and named "Stability Index". It can characterize all settling behaviors. This Stability Index corresponds to the area difference, on backscattered profiles, between profiles at 0 and $t = 6$ min. The settling time at $t = 6$ min has been chosen arbitrarily, in order to exhibit maximum differences between systems at the beginning of sedimentation phenomena.

Stability Index value, expressed in area units, is maximal when system is unstable and minimal when the system is stabilized (close to 50 area units).

On Fig. 7, a stability threshold is reached for 0.2% dosage for all suspensions studied and all superplasticizers. Note that this dosage is considerably higher than that obtained with T_{30} index (Fig. 5) when just finest particles dispersion is taken into account.

To have a better investigation for dosages below 0.2%, a different graphic representation of these results is shown on Fig. 8. Backscattered profiles at $t = 6$ min subtracted to profile at $t = 0$ min (named delta mode) are presented. Two other results could be provided: dispersion state in sediment in formation (height of sedimentation front), and mean diameter of particles in opaque supernatant (BS value - see 2.4.2.). With 8 replicates of a same formulation, standard deviations of Stability Index values have been evaluated at ±3.4% for area value, ± 5.1% for sedimentation front position and ±1.5% for BS value. Thus, different influences of macromolecular structures on particles dispersion can thus be highlighted concerning both dispersion of finest particles in supernatant (BS values) and dispersion/agglomeration phenomena in sediment in formation (sedimentation front evolution). We can see for statistical PCE that an increase in dosage leads to dispersion of all particles: sedimentation front evolution slowing down and BS value increasing. These observations are in accordance with the results of T_{30} and indicate a dispersion of finest particles as well as largest ones. But, for all other copolymers which contain phosphonic acids, the system behaves differently in particular for dosages lower than 0.1%: finest particles are still dispersed in supernatant but largest particles are destabilized as shown by the sedimentation rate values in Table 3. Destabilization increases at 0.03% and 0.01% dosages for PCE-15P and PCE-30P with sedimentation kinetics respectively of 3.34 and 2.82

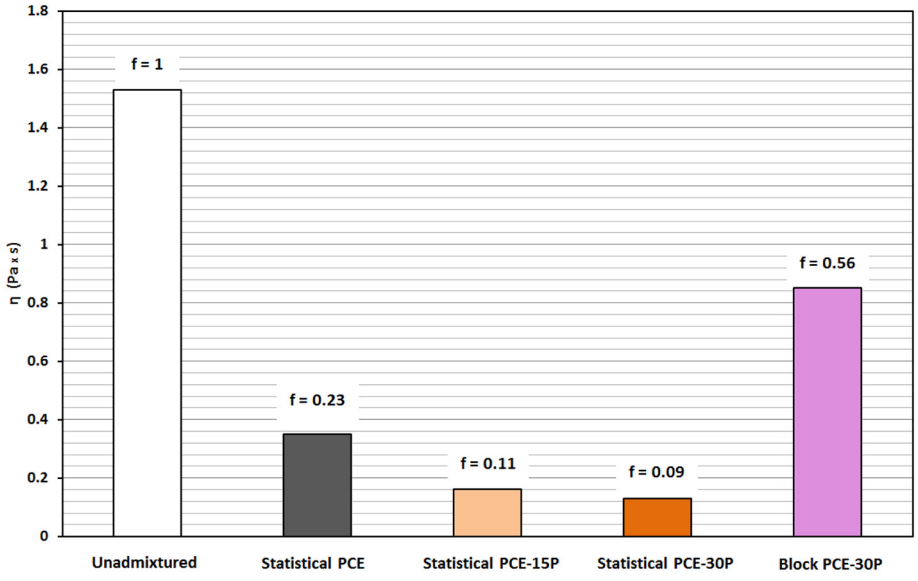

Fig. 6. Viscosities and fluidification efficiency factor of calcite suspensions according to superplasticizer employed.

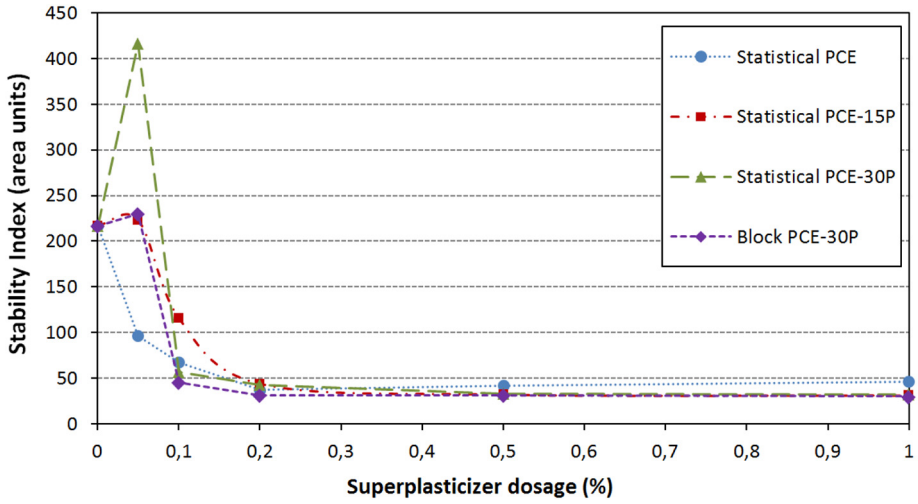

Fig. 7. Evolution of Stability Index as a function of superplasticizer dosage in limewater.

mm/min, compared with the constant value close to 2.5 mm/min for statistical PCE. For block macromolecular structure an increase in destabilization only appears at 0.05% dosage.

To conclude, finest particles dispersion and largest particles destabilization are observed at the same time in presence of phosphonic acid groups. This observation may be due to bridging phenomena arising at lowest quantity of superplasticizer adsorbed (especially the case of largest particles) [41,42] (Fig. 3) and the good adsorption ability of phosphonic acid groups on mineral surfaces [23,43].

For example, although the block PCE-30P seems to be the most effective to generally stabilize suspensions (according to Stability Index values on Fig. 8), the significant largest particles destabilization observed on Fig. 8 combined with a minor dispersion of finest particles (Fig. 5), leads to a weak fluidification (Fig. 6). For similar Stability Index and largest particles destabilization (maximum settling kinetics close to 3.4 mm/min), statistical PCE-30P presents higher finest particles dispersion which lead to higher fluidification efficiencies. These observations show the important effects of both finest particles on rheological behaviors and the complex relationships which exist between dispersion/agglomeration phenomena and macroscopic behavior of suspensions. Combined study of backscattered and transmission profiles might be an interesting way to have better understanding of involved mechanisms.

4. Conclusion

In this study, three statistical comb-like copolymers have been synthetized with different macromolecular structures. These macromolecules have similar structural parameters as molecular weight, PEO side chain length and rate of anionic functions (fixed at 30%). They just differ in the ratio of carboxylic - phosphonic acid groups. Moreover, a block copolymer has been obtained, and compared with a similar statistical structure containing 30% of phosphonic acid groups.

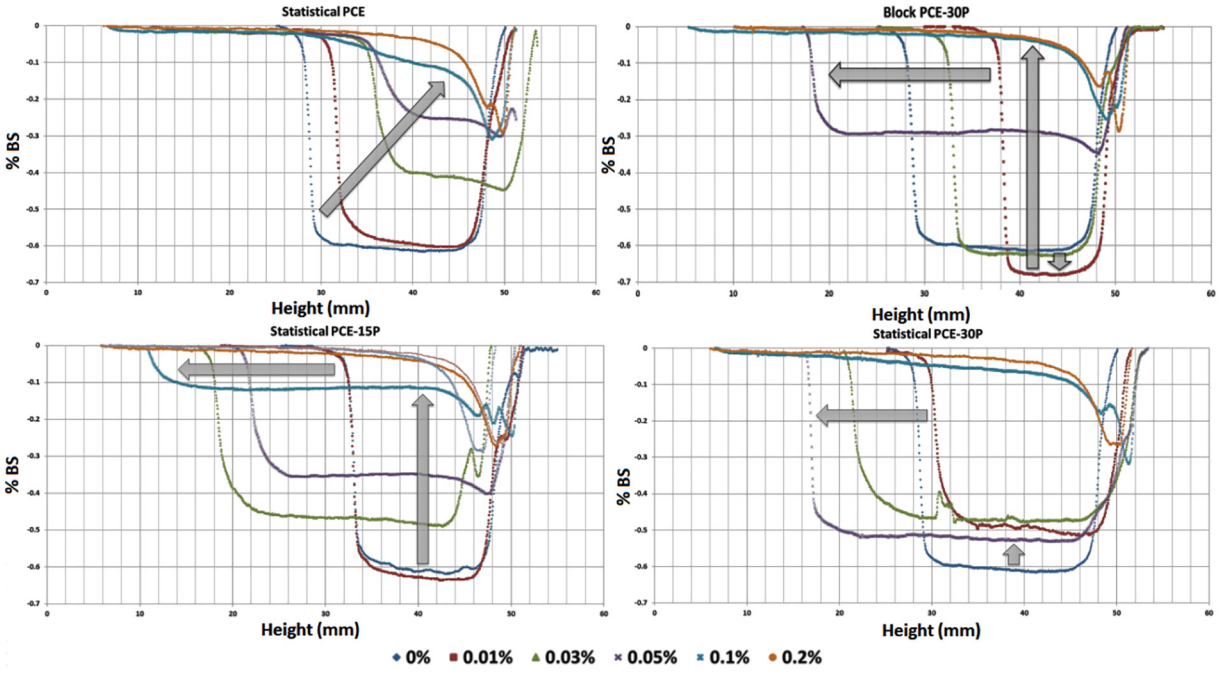

Fig. 8. Backscattered profiles at $t = 6$ min with profile at $= 0$ min subtracted (delta mode) for each copolymers at dosages between 0 and 0.2% Arrows highlight general evolutions of lowest level of backscattered intensity in turbid or opaque supernatant and sediment front position.

Table 3
Sedimentation rates as a function of superplasticizer dosage. These values are calculated from the slope of sediment front position curves as function of time, considering the 10 first minutes of settling.

	Sediment front evolution kinetics (mm/min)			
Superplasticizer dosage	Statistical PCE	Statistical PCE-15P	Statistical PCE-30P	Block PCE-30P
0%	2.48	2.49	2.47	2.47
0.01%	2.59	2.47	**2.82**	2.56
0.03%	2.49	**3.34**	**3.5**	2.47
0.05%	2.43	**3.35**	**2.97**	**3.4**

Study of their adsorption and dispersion (stability and rheological behaviors) ability has been realized onto calcium carbonate.

It can be observed that a dosage of 0.2% is needed to obtain good dispersion efficiency for all superplasticizers. However, at low dosages (up to 0.2%), addition of superplasticizer, containing phosphonic acid groups reveals:

- That an increase of phosphonic acid functions in statistical macromolecules leads to a less adsorption ability, may be due to a possible formation of polymer-Ca^{2+}complex.
- A good correlation between finest particles dispersion and fluidification efficiency shows the important role of finest particles on rheological behavior, in particular for the statistical PCE-30P which presents an important amount of phosphonic acid functions.
- Even if the block copolymer adsorbs in higher proportions, it leads to lower fluidification efficiency probably due to a different adsorbed molecule conformation (linked to polymer/solvent interactions) and/or a variable surface recovery (unknown in this work). Indeed, the study of dispersion/agglomeration shows significant destabilization of largest particles combined with a minor dispersion of finest particles. Probably, agglomeration of largest particles could be due to bridging phenomenon because copolymers adsorption is not complete.

These results show that only consider quantity of adsorbed polymer could not directly explain their impact on dispersion/agglomeration phenomena and fluidification efficiency. It's also important to take into account other parameters as adsorbed molecule conformation linked to their macromolecular structure or water soluble or insoluble complex formation. A second part of this study will investigate more superplasticizers structures, including block copolymers, and effect of an increasing of ionic strength on superplasticizers efficiencies. Work perspectives of all these researches could be to focus on polymers state in limewater, their adsorption and molecular conformation at particle-solution interphase and finally study how polymer behave in cement paste.

Acknowledgement

This work was financed by LabEx CheMISyst of Balard Chemistry Center of Montpellier and ARMINES association (Paris) from France. The authors would like to acknowledge CEA of Marcoule (France) for his contribution to this project and his financial support.

References

[1] P.-C. Aïtcin, R.J. Flatt, Science and Technology of Concrete Admixtures, Woodhead P, Elsevier Ltd., 2016
[2] J. Cheung, L. Roberts, D. Silva, A. Jeknavorian, Impact of admixtures on the hydration kinetics of Portland cement, Cem. Concr. Res. 41 (2011) 1289–1309, https://doi.org/10.1016/j.cemconres.2011.03.005.
[3] J.G. Jang, N.K. Lee, H.K. Lee, Fresh and hardened properties of alkali-activated fly ash/slag pastes with superplasticizers, Constr. Build. Mater. 50 (2014) 169–176, https://doi.org/10.1016/j.conbuildmat.2013.09.048.
[4] J. Gołaszewski, Influence of cement properties on new generation superplasticizers performance, Constr. Build. Mater. 35 (2012) 586–596, https://doi.org/10.1016/j.conbuildmat.2012.04.070.
[5] S. Hanehara, K. Yamada, Interaction between cement and chemical admixture from the point of cement hydration, absorption behaviour of admixture, and paste rheology, Cem. Concr. Res. 29 (1999) 1159–1165, https://doi.org/10.1016/S0008-8846(99)00004-6.
[6] A. Colombo, M. Geiker, H. Justnes, R.A. Lauten, K. De Weerdt, On the effect of calcium lignosulfonate on the rheology and setting time of cement paste, Cem. Concr. Res. 100 (2017) 435.
[7] M. Adjoudj, K. Ezziane, E. Hadj, T. Ngo, A. Kaci, Evaluation of rheological parameters of mortar containing various amounts of mineral addition with polycarboxylate superplasticizer, Constr. Build. Mater. 70 (2014) 549–559, https://doi.org/10.1016/j.conbuildmat.2014.07.111.
[8] C.A. Anagnostopoulos, Effect of different superplasticisers on the physical and mechanical properties of cement grouts, Constr. Build. Mater. 50 (2014) 162–168, https://doi.org/10.1016/j.conbuildmat.2013.09.050.
[9] M. Courtial, M.N. De Noirfontaine, F. Dunstetter, M. Signes-Frehel, P. Mounanga, K. Cherkaoui, Effect of polycarboxylate and crushed quartz in UHPC: microstructural investigation, Constr. Build. Mater. 44 (2013) 699–705, https://doi.org/10.1016/j.conbuildmat.2013.03.077.
[10] A.K.H. Kwan, W.W.S. Fung, Effects of SP on flowability and cohesiveness of cement-sand mortar, Constr. Build. Mater. 48 (2013) 1050–1057, https://doi.org/10.1016/j.conbuildmat.2013.07.065.
[11] B. Ma, M. Ma, X. Shen, X. Li, X. Wu, Compatibility between a polycarboxylate superplasticizer and the belite-rich sulfoaluminate cement: setting time and the hydration properties, Constr. Build. Mater. 51 (2014) 47–54, https://doi.org/10.1016/j.conbuildmat.2013.10.028.
[12] Y. Li, Y. Zhang, J. Zheng, H. Guo, C. Yang, Z. Li, M. Lu, Dispersion and rheological properties of concentrated kaolin suspensions with polycarboxylate copolymers bearing comb-like side chains, J. Eur. Ceram. Soc. 34 (2014) 137–146, https://doi.org/10.1016/j.jeurceramsoc.2013.07.009.
[13] J. Plank, E. Sakai, C.W. Miao, C. Yu, J.X. Hong, Chemical admixtures — chemistry, applications and their impact on concrete microstructure and durability, Cem. Concr. Res. 78 (2015) 81–99, https://doi.org/10.1016/j.cemconres.2015.05.016.
[14] K. Yamada, T. Takahashi, S. Hanehara, M. Matsuhisa, Effects of the chemical structure on the properties of polycarboxylate-type superplasticizer, Cem. Concr. Res. 30 (2000) 197–207, https://doi.org/10.1016/S0008-8846(99)00230-6.
[15] C.Z. Li, N.Q. Feng, Y. De Li, R.J. Chen, Effects of polyethlene oxide chains on the performance of polycarboxylate-type water-reducers, Cem. Concr. Res. 35 (2005) 867–873, https://doi.org/10.1016/j.cemconres.2004.04.031.
[16] Q. Ran, P. Somasundaran, C. Miao, J. Liu, S. Wu, J. Shen, Effect of the length of the side chains of comb-like copolymer dispersants on dispersion and rheological properties of concentrated cement suspensions, J. Colloid Interface Sci. 336 (2009) 624–633, https://doi.org/10.1016/j.jcis.2009.04.057.
[17] K. Yamada, S. Ogawa, S. Hanehara, Controlling of the adsorption and dispersing force of polycarboxylate-type superplasticizer by sulfate ion concentration in aqueous phase, Cem. Concr. Res. 31 (2001) 375–383, https://doi.org/10.1016/S0008-8846(00)00503-2.
[18] C. Jolicoeur, M.-A. Simard, Chemical admixture-cement interactions: phenomenology and physico-chemical concepts, Cem. Concr. Compos. 20 (1998) 87–101, https://doi.org/10.1016/S0958-9465(97)00062-0.
[19] A. Habbaba, Z. Dai, J. Plank, Formation of organo-mineral phases at early addition of superplasticizers: the role of alkali sulfates and C3A content, Cem. Concr. Res. 59 (2014) 112–117, https://doi.org/10.1016/j.cemconres.2014.02.007.
[20] W. Fan, F. Stoffelbach, J. Rieger, L. Regnaud, A. Vichot, B. Bresson, N. Lequeux, A new class of organosilane-modified polycarboxylate superplasticizers with low sulfate sensitivity, Cem. Concr. Res. 42 (2012) 166–172, https://doi.org/10.1016/j.cemconres.2011.09.006.
[21] S. Pourchet, S. Liautaud, D. Rinaldi, I. Pochard, Effect of the repartition of the PEG side chains on the adsorption and dispersion behaviors of PCP in presence of sulfate, Cem. Concr. Res. 42 (2012) 431–439, https://doi.org/10.1016/j.cemconres.2011.11.011.
[22] B. Felekoğlu, H. Sarikahya, Effect of chemical structure of polycarboxylate-based superplasticizers on workability retention of self-compacting concrete, Constr. Build. Mater. 22 (2008) 1972–1980, https://doi.org/10.1016/j.conbuildmat.2007.07.005.
[23] F. Dalas, A. Nonat, S. Pourchet, M. Mosquet, D. Rinaldi, S. Sabio, Cement and concrete research tailoring the anionic function and the side chains of comb-like superplasticizers to improve their adsorption, Cem. Concr. Res. 67 (2015) 21–30, https://doi.org/10.1016/j.cemconres.2014.07.024.
[24] A.M. Kjeldsen, R.J. Flatt, L. Bergström, Relating the molecular structure of comb-type superplasticizers to the compression rheology of MgO suspensions, Cem. Concr. Res. 36 (2006) 1231–1239, https://doi.org/10.1016/j.cemconres.2006.03.019.
[25] Y.F. Houst, P. Bowen, F. Perche, A. Kauppi, P. Borget, L. Galmiche, J.F. Le Meins, F. Lafuma, R.J. Flatt, I. Schober, P.F.G. Banfill, D.S. Swift, B.O. Myrvold, B.G. Petersen, K. Reknes, Design and function of novel superplasticizers for more durable high performance concrete (superplast project), Cem. Concr. Res. 38 (2008) 1197–1209, https://doi.org/10.1016/j.cemconres.2008.04.007.
[26] L. Ferrari, J. Kaufmann, F. Winnefeld, J. Plank, Multi-method approach to study influence of superplasticizers on cement suspensions, Cem. Concr. Res. 41 (2011) 1058–1066, https://doi.org/10.1016/j.cemconres.2011.06.010.
[27] N. Mikanovic, C. Jolicoeur, Influence of superplasticizers on the rheology and stability of limestone and cement pastes, Cem. Concr. Res. 38 (2008) 907–919, https://doi.org/10.1016/j.cemconres.2008.01.015.
[28] Z.E.L. Asri, K. Chougrani, C. Negrell-guirao, G. David, B. Boutevin, An Efficient Process for Synthesizing and Hydrolyzing a Phosphonated Methacrylate: Investigation of

the Adhesive and Anticorrosive Properties, 2008 4794–4803, https://doi.org/10.1002/pola.
[29] B. Canniccioni, S. Monge, G. David, J. Robin, Polymer Chemistry PAPER RAFT Polymerization of Dimethyl (Methacryloyloxy) - A New Opportunity for Phosphorus-Based Materials, 2013 3676–3685, https://doi.org/10.1039/c3py00426k.
[30] O. Mengual, G. Meunier, I. Cayre, K. Puech, P. Snabre, Characterisation of instability of concentrated dispersions by a new optical analyser: the TURBISCAN MA 1000, Colloids Surf. A Physicochem. Eng. Asp. 152 (1999) 111–123, https://doi.org/10.1016/S0927-7757(98)00680-3.
[31] C. Autier, N. Azéma, J.M. Taulemesse, L. Clerc, Mesostructure evolution of cement pastes with addition of superplasticizers highlighted by dispersion indices, Powder Technol. 249 (2013) 282–289, https://doi.org/10.1016/j.powtec.2013.08.036.
[32] C. Autier, N. Azéma, P. Boustingorry, Using settling behaviour to study mesostructural organization of cement pastes and superplasticizer efficiency, Colloids Surf. A Physicochem. Eng. Asp. 450 (2014) 36–45, https://doi.org/10.1016/j.colsurfa.2014.02.050.
[33] B. Yu, Z. Zeng, Q. Ren, Y. Chen, M. Liang, H. Zou, Study on the performance of polycarboxylate-based superplasticizers synthesized by reversible addition-fragmentation chain transfer (RAFT) polymerization, J. Mol. Struct. 1120 (2016) 171–179, https://doi.org/10.1016/j.molstruc.2016.05.035.
[34] S. Pourchet, I. Pochard, F. Brunel, D. Perrey, Chemistry of the calcite/water interface: influence of sulfate ions and consequences in terms of cohesion forces, Cem. Concr. Res. 52 (2013) 22–30, https://doi.org/10.1016/j.cemconres.2013.04.002.
[35] Thomas M. Riddick, Control of Colloid Stability Through Zeta Potential and its Relationship to Cardiovascular Disease(Published for Zeta-Meter, Inc.) Livingston Pub. Co., 1968
[36] F. Dalas, S. Pourchet, A. Nonat, D. Rinaldi, S. Sabio, M. Mosquet, Fluidizing efficiency of comb-like superplasticizers: the effect of the anionic function, the side chain length and the grafting degree, Cem. Concr. Res. 71 (2015) 115–123, https://doi.org/10.1016/j.cemconres.2015.02.001.
[37] M. Bishop, S.G. Bott, A.R. Barron, A new mechanism for cement hydration inhibition: solid-state chemistry of calcium nitrilotris(methylene)triphosphonate, Chem. Mater. 15 (2003) 3074–3088, https://doi.org/10.1021/cm0302431.
[38] C. Schröfl, M. Gruber, J. Plank, Preferential adsorption of polycarboxylate superplasticizers on cement and silica fume in ultra-high performance concrete (UHPC), Cem. Concr. Res. 42 (2012) 1401–1408, https://doi.org/10.1016/j.cemconres.2012.08.013.
[39] R.J. Flatt, I. Schober, E. Raphael, C. Plassard, E. Lesniewska, Conformation of adsorbed comb copolymer dispersants, Langmuir 25 (2009) 845–855, https://doi.org/10.1021/la801410e.
[40] Z.C. Chen, T.A. Ring, J. Lemaître, Stabilization and processing of aqueous $BaTiO_3$ suspension with polyacrylic acid, J. Am. Ceram. Soc. 75 (1992) 3201–3208, https://doi.org/10.1111/j.1151-2916.1992.tb04412.x.
[41] H. Huang, E. Ruckenstein, The bridging force between colloidal particles in a polyelectrolyte solution, Langmuir 28 (2012) 16300–16305, https://doi.org/10.1021/la303918p.
[42] F. Lafuma, K. Wong, B. Cabane, Bridging of colloidal particles through adsorbed polymers, J. Colloid Interface Sci. 143 (1991) 9–21, https://doi.org/10.1016/0021-9797(91)90433-9.
[43] M. Mosquet, Y. Chevalier, S. Brunel, J.P. Guicquero, P. Le Perchec, Polyoxyethylene diphosphonates as efficient dispersing polymers for aqueous suspensions, J. Appl. Polym. Sci. 65 (1997) 2545–2555, https://doi.org/10.1002/(SICI)1097-4628(19970919)65:12<2545::AID-APP24>3.0.CO;2-Y.